A Hybrid Scheme for SAR Computation of Human Head and the Resulting Performance Evaluation of MIMO Systems in the Context of Electromagnetic Asymmetry

V. Rama Krishna Sharma*, Dr. Chandrasekhar Paidimarri **

* *Associate Professor, ECE Department, GNI, Hyderabad*
** *HEAD, ECE Department, Osmania University, Hyderabad*

Abstract

In recent years, ever-increasing proliferation of handheld terminals has served to enhance the level of concern for possible deleterious biological effects of electromagnetic waves absorbed by the human body. The influence of surrounding environment caused by EM radiation is always a serious problem. Scientists use the SAR (specific absorption rate) to determine the amount of radiation that human tissue absorbs. This measurement is especially important for mobile telephones, which radiate close to the brain. Over the last decade, the Specific Absorption Rate (SAR) value has been used as the standard dosimetric parameter in defining the energy absorbed by the human body exposed to electromagnetic radiation. This paper evaluates affects of near-field exposure, specifically the SAR values induced by the cellular Multi- Input Multi-Output (MIMO) antenna and also models how a human head absorbs a radiated wave from an antenna and the temperature increase that the absorbed radiation causes.

1. Introduction

when the cellular mobile radio system is functioning, and the transmitting terminal is located in close proximity of the human head − say less than 7 mm − a large fraction of the power radiated by the mobile radio is absorbed by the user. particular, in the RF and microwave frequency bands, the absorbed Elctro-magnetic (EM) energy mainly contributes to the heating of the tissues[1]. The value of 4W/kg is accepted worldwide as the threshold for the induction of biological thermal effects[2]. Scientists use the SAR (specific absorption rate) to determine the amount of radiation that human tissue absorbs. This measurement is especially important for mobile telephones, which radiate close to the brain. The increasing use of wireless equipment has also increased the amount of radiation energy to which human bodies are exposed, and it is particularly important to avoid radiation into the brain. Experts continue to debate how dangerous this radiation might be. The reduction in the radiation efficiency of an antenna in a mobile handset due to user's hand effects is of importance. A parameter called body loss is defined to evaluate the degradation of the radiation efficiency. The interactions between the antenna in a mobile terminal and the user's body can lead to impedance mismatch and reduce the radiation efficiency of the antenna dramatically, which will reduce the channel's data rate.

2. Contextual Evaluation Of MIMO System

The structure of cellular phone, shown in Fig.1, is a MIMO system, which employs a technology that is different from the smart antenna technology, also referred to as the beam-forming technology. It employs multiple transmitters to send separate message and multiple terminals to receive separate message in the same radio channel, and then applies advanced digital signal process (DSP) algorithm in the MIMO decoder. The MIMO system makes full usage of multipath transmission effects to overcome multipath fading effects [3]. Fig.2 shows the MIMO system, in which the data are sent by different transmitters in different parts, while in the smart phone system, depicted in the same figure, all of the transmitting terminals in smart antenna technology send the same data. The dimensions of the handheld phone are

108×65.5×13.5mm along x -, y- and z-axes, respectively. It consists of three parts: antenna system; battery; and, the LED display and its cover. The geometrical parameters of the cellular phone are shown in Table1. As is well known, the coupling between the different receivers in a MIMO system is a cause for concern, since the system performance of MIMO deteriorates as the coupling becomes high, and the system eventually fails for very high levels of coupling.

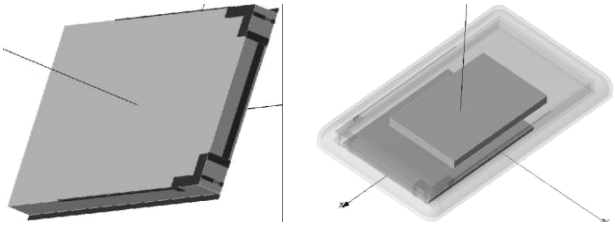

(a) Antenna only
(b) Antenna with LED, battery and cover

Fig 1: a & b – 3-D View of cellular antenna system

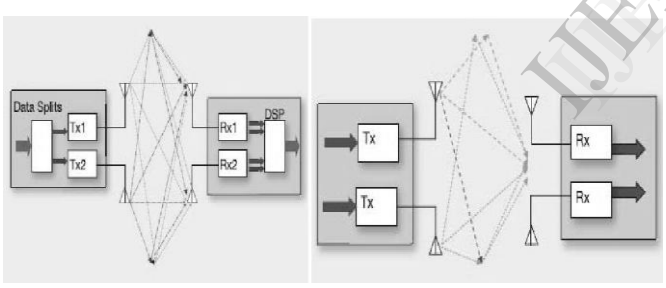

Fig 2: MIMO wireless system

3. EM Heating of the Head & Perfusion Rate

The heat loss depends on the heat capacity and density of the blood, and on the blood perfusion rate. The perfusion rate varies significantly in different parts of the human body, and the table below presents the values used here.

PART	PERFUSION RATE
Brain	$2{\cdot}10^{-3}$ (ml/s)/ml
Bone	$3{\cdot}10^{-4}$ (ml/s)/ml
Skin	$3{\cdot}10^{-4}$ (ml/s)/ml

Table 1: perfusion rates of different parts of head

The same interpolation function used for the electric parameters also models the difference in perfusion rate between the brain tissue inside the head and the outer parts of skin and bone. Note again that the use of the interpolation function does not have any physical relevance; it is just to show a realistic effect of a varying material parameter. The differences in electrical properties become visible if you plot the local SAR value on a log scale (Fig 3).

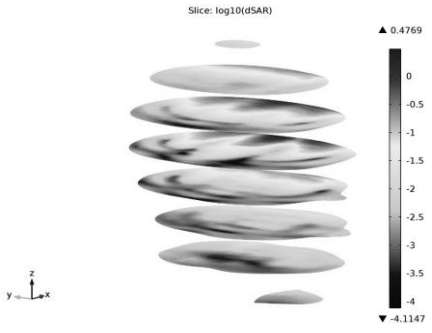

Fig 3: Log-scale slice plot of the local SAR value

4. SAR Computation for Human Head

The SAR is expressed as:

$$SAR = \frac{\sigma \left| E \right|^2}{\rho} \qquad (1)$$

where σ is the electrical conductivity (in S/m), |E| is the root mean square (rms) magnitude of the

electric field strength vector (in V/m) and ρ is the mass density of the tissue (in kg/m3)[4]. Recent work has provided the validation of GEMS in calculating the SAR values based on the IEEE 1528 (2003) standard. We take advantage of this in the present work, and also employ GEMS, a parallel-FDTD algorithm, to compute the SAR values of interest. We begin by placing the hand-held antenna near the SAM head model to evaluate the SAR values in free-space. The SAM head model is 260×256×174 mm along x-, y- and z-coordinates, respectively, and is composed of two parts: the inner region, which is filled with an appropriate liquid; the enclosure, which is the skull modeled by a dielectric shell, covered by a 5mm thick skin-like material. The relevant parameters for the head model are presented in Table 2.

Property	Name	Value
Thermal conductivity	k	0.5
Density	rho	1050
Heat capacity at constant pressure	Cp	3700
Relative permittivity	epsilonr	epsilonr_brain
Relative permeability	mur	1
Electric conductivity	sigma	sigma_brain

Table 2: properties and their approximated values considered for analysis

5. Performance Evaluation in the Context of EM Asymmetry

The relative positions of the antenna, SAM head phantom and PDA hand phantom in the talking mode and the data mode strictly follow the CTIA standard [5]. The OG PIFA can be placed in three positions where the specific absorption rate (SAR) is smaller than 1.6 W/kg in accordance with the 1 g standard. These three positions are shown in Figure 4 (the hand and antenna case box are hidden in Figure 4 in order to show different positions more clearly).

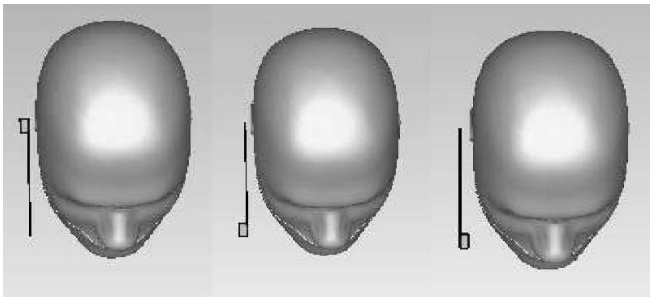

Fig 4: Three different positions of OG PIFA on the right side of the head phantom

6. Discussion of Simulated Results and Conclusion

The antenna's operation bands are presented in Figure 5(a), with the consideration of the right or left hand effects. When the antenna is mounted on the top of ground plane, the left-and-right-hand difference is due to the impact of the index finger, and when the antenna is mounted on the bottom of the ground plane, this difference is mainly caused by that the antenna is covered by different parts of hand phantom (either the bottom part of the thumb or the tip of the little finger) [6]. It can be observed that in the lower band the left- and right-hand effects in all three positions are similar, but position 3 can provide better radiation efficiencies for both hands. In the higher band, position 3 has a higher efficiency and less difference between the left-and right-hand cases than positions 1 and 2. Therefore, it is more meaningful to improve further the radiation efficiencies (for both left and right hands) in position 3. In addition, the low radiation efficiency and large difference between the left and right hands in position 1 are mainly due to the impact of the index finger. In [7], the switching method is adapted for co-located multi antenna systems to reduce the influence of the index finger on the antenna's efficiency. However, for the single antenna or the top antenna in a separately located MIMO array it is quite challenging to enhance the worst performance of the antenna's radiation efficiency and reduce the difference between the left- and right-hand cases in radiation efficiencies. Thus, the position 3 is adapted in the following study. In order to demonstrate the feasibility of position 3 in mobile handset, the SAR value is examined. The SAR (according to the 1 g standard) performance of position 3 is plotted in Figure 5(b), where we set the accepted power of the antenna to a constant value of 23 dBm in order to eliminate the influence of the mismatch loss when the antenna is close to the head phantom. The 23 dBm

is the maximum output power of the LTE mobile handset [8], and the SAR value we get is for the worst performance of our proposed antenna in position 3. Nevertheless, it can be observed that the SAR values in all operation bands are much smaller than the limitation (1.6 W/kg).

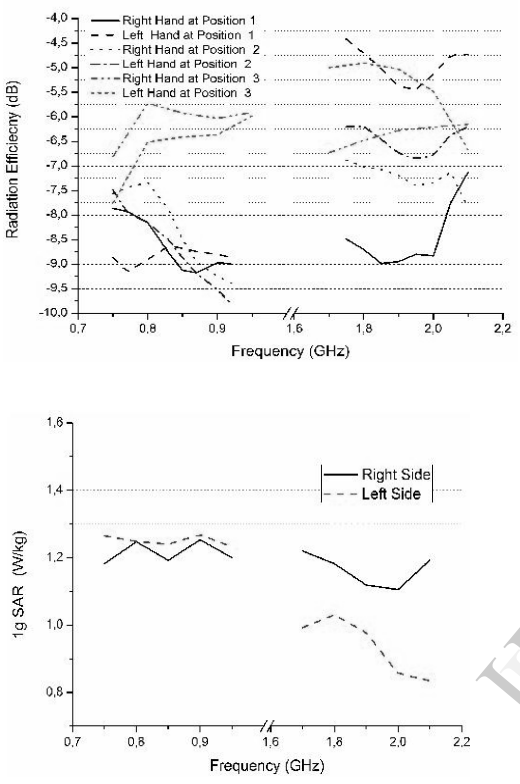

Fig 5: (a) The radiation efficiencies of our antenna in the talking mode

(b) SAR Value of position 3 on the left or right side of the hand phantom

The degradation of the radiation efficiency in the higher band (1.7 GHz to 2.1 GHz) is more severe for position 3, especially with the right hand; the radiation efficiency on the right hand is 2 dB lower than on the left hand on average. Based on the above analysis, we know that the density of the power loss in the higher band (from 1.7 GHz to 2.1 GHz) is mainly from the bottom of the thumb and the tip of the little finger. Therefore, we try to enlarge the distance between the higher band radiator of our antenna and any of these two parts on a hand.

Fig 6: The body loss in the talking mode.

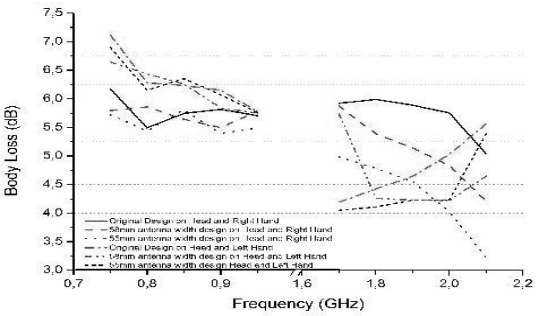

Fig 7: The body loss in the data mode

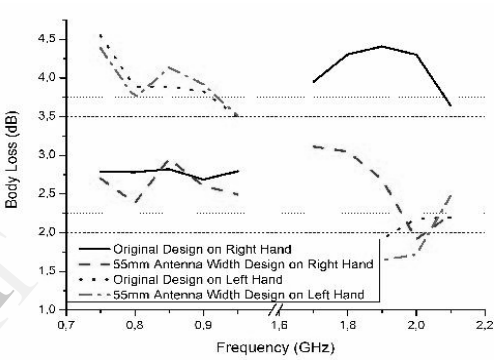

The body loss of the original antenna (60 mm width) and the modified antennas (58 mm or 55 mm width) are plotted in Figure 6. With the smaller antenna width, we can observe that in the higher band, the body loss can be reduced by about 1.5 dB for the right-hand case with 55 mm width. For the left-hand case, the reduction of the body loss in the higher band is similar (which is around 0.5 dB on average) whether the antenna width is reduced to 58 mm or 55 mm. Meanwhile, the body losses are also optimized in the lower band, especially when the width of the antenna is reduced to 55 mm, the body loss can be reduced by as much as 0.3 dB for the right-hand case at some frequency points. The antenna design with reduced 55 mm antenna width is also tested on the data mode (single PDA hand). The body losses of the original and modified designs are shown in Figure 7.

Our model studies the local SAR value in the head using the formula described earlier for the frequency 835 MHz. The SAR value is highest close to the surface of the head facing the incident wave. The bio-heat equation produces a similar plot for the heating of the head, which is highest closest

Material Parameter	Relative Permitivity (ε_r)	Tangential Loss(tanδ)	Conductivity σ (S/m)	Density (g/cm^3)
Vacuum	1		0	0
Dielectric	2.6	0.01		0
Cover	4.4	0.02		0
Inner of SAM model @2.4GHz	5		0.0125	1
Outer of SAM model @2.4GHz	39		1.89	1
Copper	1		5×10^7	1

to the antenna. The maximum temperature increase (from 37 deg C) is less than 0.2 deg C, and drops rapidly inside the head.

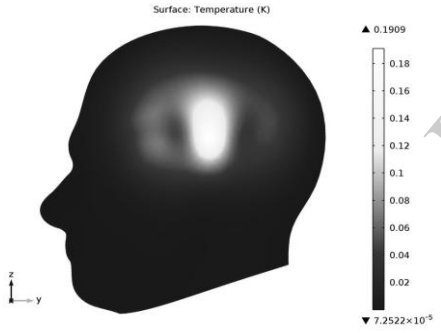

Fig 8: The local increase in temperature at the surface has a maximum of 0.193 deg C right beneath the antenna

Our objective in this paper is to estimate the 1g and 10g SAR values of SAM head model for different scenarios, namely when the head model is located in free-space, as well as when it is placed inside a car model. Tables 4 and 5, present the computed both the 1g and 10g SAR values, and we note that those in Table 4 are higher than the corresponding ones in Table 5. This is because the location of port-1 of the antenna is much closer to the ear of the SAM head model as compared to that of port-2. We note, further, that both the 10g SAR and 1g SAR levels change little, when the head model is located inside the model car. This, in turn, leads us to conclude that the electromagnetic environment of the car has very little effect on the estimated SAR values.

Table 3: Parameters of Cellular phone and SAM models.

SAR(W/KG)/ Freq (GHz)	Max.SAR	1g SAR	10g SAR
2.2	22.27	13.19	6.67
2.4	21.04	12.77	6.70

Table 4: SAR Values when port1 of cell is working.

SAR(W/KG)/ Freq (GHz)	Max.SAR	1g SAR	10g SAR
2.2	12.77	6.19	3.55
2.4	11.60	5.56	3.22

Table 5: SAR Values when port 2 of cell is working

Model Frequency (GHz)	SAM only	SAM head model in car
2.255	13.19	12.26
2.4	12.77	10.70

Table 6: 1g SAR values for two cases when only port-1 of cellular antenna excited.

Model Frequency (GHz)	SAM only	SAM head model in car
2.255	6.67	6.13
2.4	6.70	5.70

Table 7: 10g SAR values for two cases when only port-1 of cellular antenna excited

Three different positions of the LTE antenna in the talking mode have been discussed, and position 3 has been recommended based on the performance of radiation efficiency. In order to reduce further the hand-effect body loss in the talking and data modes, a modified design with a smaller width of the antenna has been proposed and the body loss performance with different values of antenna width

has been studied. The test has been carried out in both the talking and data modes from CTIA standard. With our modified design, the body loss for both hands can be optimized, especially for the right hand. In this paper, we evaluate the effects of near-field exposure, specifically the SAR values induced by the cellular Multi- Input Multi-Output (MIMO) antenna. Towards this end, we employ the Specific Anthropomorphic Mannequin (SAM) Head Model, comprised of a low-loss dielectric material.

Appendix

Name	Expression	Description
epsilonr_pcb	5.23	Permittivity for the patch antenna board
epsilonr0_brain	56	Permittivity for the brain Tissue
sigma0_brain	1.35[S/m]	Conductivity for the brain tissue
rho_brain	1.03e3[kg/m^3]	Density of brain Tissue
sdamping	2e-4	Sampling parameter
edamping	4e-4	Sampling parameter
eoffset	-50	Sampling parameter
c_blood	3639[J/(kg*K)]	Heat capacity of blood
rho_blood	1000[kg/m^3]	Density of blood
odamping	1.08e-6[1/s]	Sampling parameter
ooffset	7.8e-4[1/s]	Sampling parameter
freq	835[MHz]	Frequency

References

[1] Toshihiro Togashi, Tomoaki Nagaoka, Satoru Kikuchi, Kazuyuki Saito, Soichi Watanabe, Masaharu Takahashi, and Koichi Ito, "FDTD Calculations of Specific Absorption Rate in Fetus Caused by Electromagnetic Waves From Mobile Radio Terminal Using Pregnant Woman Model," *IEEE Transactions on Microwave Theory and Techniques*, Volume56, Issue2, pp554 – 559, Feb. 2008.

[2] Paolo Bernardi, Marta Cavagnaro, Stefano Pisa, Member, and Emanuele Piuzzi, "Specific absorption rate and temperature increases in the head of a cellular-phone user," *IEEE Transactions on Microwave Theory and Techniques*, Volume48, Issue7, pp1118 – 1126, Jul 2000.

[3] Fan Liang, "The challenges of testing MIMO," *Next-Generation Wireless*, Nov. 2005

[4] IEEE Standards Coordinating Committee 34, "1528TM *IEEE Recommended Practice for Determining the Peak Spatial-Average Specific Absorption Rate (SAR) in the Human Head from Wireless Communications Devices: Measurement Techniques*," 2003

[5] Test plan for the mobile station over the air performance," *CTIA*, 2010.

[6] Li, C.-H., E. O°, N. Chavannes, E. Cherubini, H. U. Gerber, and Kuster, Effects of hand phantom on mobile phone antenna performance," *IEEE Trans. Antennas Propag.*, Vol. 57, No. 9, 2763{2770, Sep. 2009.

[7] Ramanchanran, P., Z. Milosavjevic, and C. Beckman, \Adaptive penta-band handset antenna with hand effect compensation," *IEEE Microwaves, Antennas & Propagation*, Vol. 6, No. 1, 79{86, Jan. 2011.

[8] 3GPP TS 36.101 v11.2.0 (2012.09) *http://www.3gpp.org/ftp/Sp-ecs/archive/36 series/36.101/.*